Desalination and Water Treatment
www.deswater.com
doi: 10.5004/dwt.2023.29721

300 (2023) 57–64
July

Tellurium-cobalt/polybutylene terephthalate nanocomposites: preparation, analysis and photocatalytic application

Tamanna Gul, Khalid Saeed*, Navidullah

Department of Chemistry, Bacha Khan University, Charsadda, KP, Pakistan, emails: khalidkhalil2002@yahoo.com/ khalidsaeed@bkuc.edu.pk (K. Saeed), tamannakhan8224@gmail.com (T. Gul), unavid6@gmail.com (Navidullah)

Received 31 December 2022; Accepted 7 June 2023

ABSTRACT

Tellurium-cobalt/polybutylene terephthalate (Te-Co/PBT) and Te/PBT nanocomposites were prepared via solution casting method. The morphological study presented that both Te and Te-Co nanoparticles (NPs) are well embedded inside the polymer matrix. The Te NPs are round in shape having size less than 150 nm. While Te-Co NPs are in agglomerated form. The size of agglomerated NPs are below 400 nm. The formation of NPs was also confirmed by Fourier-transform infrared spectroscopy and energy-dispersive X-ray spectroscopy. thermogravimetric analysis presented that the thermal stability of nanocomposites was higher than neat PBT. Photodegradation study presented that the Te-PBT and Te-Co/PBT nanocomposites significantly degraded the bromothymol blue dye in aqueous medium. The neat PBT degraded about 7% and 21% of dye while Te(40 wt.%)/PBT and Te/Co(40 wt.%)/PBT degraded about 51% and 71%, and 56% and 77% dye, respectively within 2 and 8 h irradiation time.

Keywords: Bromothymol blue; Nanoparticles; Polybutylene terephthalate; Nanocomposite; Photodegradation

1. Introduction

Polymer based composites are considered as heterogeneous systems that comprise of a polymer matrix and fillers such as carbon nanotubes, nanoclay, graphene, metallic nanoparticles, activated carbon etc. [1]. The majority of polymeric materials are non-conducting, low mechanical, thermal and optical properties, which may be enhanced by the incorporation of fillers like metallic nanoparticles, carbon fibres, carbon nanotubes, nanoclay, graphite etc. For example, Saeed et al. [2] prepared Co–Mn/nylon-6,6 nanocomposites via solution casting method. They found that the thermal and mechanical properties of nylon-6,6 were increased by the addition of Co–Mn NPs into the polymeric matrix. Ullah et al. [3] prepared illite/polycaprolactone/ zein electrospun scaffolds. They found that the incorporation of illite clay enhanced the mechanical properties of composite scaffolds. Further, they reported that the clay-corn-caprolactone scaffold is a promising material for bone tissue engineering. Thompson et al. [4] incorporated branched carbon nanotubes into polybutylene terephthalate, which significantly improved both the storage and loss modulus of polybutylene terephthalate (PBT).

Recent years have seen increased effluents discharge due to the high usage of organic dyes in the leather, cosmetic, food and textile industries, resulting in increased water contamination. Due to their large size, complex structure, chemical stability and poor biodegradability, majority of organic dyes in wastewater, have trouble being degraded [5]. These dyes not only disturb the ecosystem but also cause serious toxic problems in plants, animals and human beings. The presence of these coloring materials in water also retard sunlight penetration in the water and disturb aquatic life [6]. Various techniques have been used to control the water pollution caused by dyes, including adsorption, ozonation, ultrafiltration, electrochemical methods, bioremediation,

* Corresponding author.

enzymatic processes, and photocatalysis [7–9]. Among these techniques, photocatalysis has advantages over other methods due to effectiveness, non-selective oxidation, low cost and environmentally friendly way of removing contaminates/pollutants from water [10]. Photocatalytic degradation occurs when photocatalyst expose to light, which absorbs photons with an energy equal to or greater than its bandgap energy and results the excitation of electrons occur from valence band to conduction band in the semiconductor. The electrons react with dissolve oxygen to generate $O_2^{\bullet}$ while positive charge holes react with water to form $OH^{-\bullet}$ radicals. Both hydroxyl and super oxide anion radicals are strong oxidizing agent, react with organic dyes and lead to their degradation [11,12].

In the current study, Te-PBT and Te-Co/PBT nanocomposites were prepared via solution casting method. The polymer-based nanocomposites were analyzed by various instrumental techniques such as scanning electron microscopy (SEM), energy-dispersive X-ray spectroscopy (EDX), Fourier-transform infrared spectroscopy (FTIR) and thermogravimetric analysis (TGA). The prepared polymer-based nanocomposites were also employed as catalyst for the photodegradation bromothymol blue (BTB) dye in aqueous medium.

2. Experimental set-up

2.1. Materials

Polybutylene terephthalate (PBT), formic acid, cobalt chloride and tellurium powder were obtained from Sigma-Aldrich (Germany). The bromothymol blue dye was received from Fisher Chemical (United States).

2.2. Preparation of tellurium/cobalt (Te/Co) NPs

100 mL $CoCl_2$ (0.1 M) and 1 g of Te powder was taken in flask and then added 0.2 M NaOH dropwise until the pH of the mixture reached to basic medium. The mixture was reflexed at 60°C for 2 h. After specific reaction time, the mixture was cooled and Te/Co NPs were obtained via filtration. The NPs were oven dried and stored.

2.3. Preparation of Te/Co/PBT nanocomposite

0.12 g Te/Co NPs was added in PBT solution (PBT dissolved in tetrahydrofurane), stirred for 2 h and then sonicated for 15 min. The viscous solution of Te-Co(8 wt.%)/PBT film/sheet was prepared via solution casting method. The obtained film of Te-Co(8 wt.%)/PBT was washed several times with distilled water in order to remove any attach trifluoroacetic acid. The same method was also adopted for the preparation of 16, 24, 32 and 40 wt.% Te/Co/PBT and Te/PBT nanocomposites films/sheets.

2.4. Photodegradation of bromothymol blue

10 mL BTB dye (120 ppm) solution was taken in various beakers and 0.03 g of each Te/PBT and Te/Co/PBT nanocomposites were separately added to each beaker. The mixture solutions were kept in dark for 20 min and then irradiated under UV light for specific time. The samples were continuously stirred during UV irradiation. After specific irradiation time, the nanocomposite was separated from dye solution and BTB degradation was analyzed by UV-Vis spectrophotometer. Percent photodegradation study of PBT was carried out using the following equations:

$$\text{Degradation rate}(\%) = \left(\frac{C_0 - C}{C_0}\right) \times 100$$

$$\text{Degradation rate}(\%) = \left(\frac{A_0 - A}{A_0}\right) \times 100$$

where C_0 indicates dye initial concentration, C indicates the concentration of dye after UV irradiation. A_0 indicates initial dye concentration while A is the absorbance of dye after UV radiation.

2.5. Instrumentation

FTIR study of PBT, Te/PBT and Te/Co/PBT nanocomposites was performed by FTIR spectrometer (PerkinElmer, Serial Number 95120, UK). SEM and EDX analysis of Te/PBT and Te/Co/PBT nanocomposites of fractured surface was carried out by SEM LA-6490, JEOL, Japan (energy range of 0–20 keV) and EDX-INCA 200/Oxford Instruments, Oxford, UK, respectively. Thermogravimetric analysis was performed in a nitrogen atmosphere at a heating rate of 10°C/min from room temperature to 600°C using TGA (TGA-50 Shimadzu). The photodegradation study of BTB was conducted using UV-Vis spectrophotometer (Model UV-1800, Shimadzu, Japan).

3. Results and discussion

3.1. FTIR study

Figs. 1 and 2 show the FTIR spectra of PBT, Te/PBT and Co-Te/PBT nanocomposites. The FTIR spectrum of PBT presented a broad peak at 3,500–3,200 cm^{-1}, which might be due to the stretching vibration of OH group [13]. The peaks appeared at about 2,930 and 1,720 cm^{-1} are due to the stretching vibration of C–H and C=O. The PBT spectrum show bands at 1,455 and 1,405 cm^{-1}, which correspond to the bending vibrations of methylene groups and stretching vibration of C–C in the benzene rings, respectively. The peaks appeared in the region 1,150 and 1,000 cm^{-1} might be due to the C–O–C stretching vibration. The spectra also showed peaks at about 725 and 555–395 cm^{-1}, which might be due to the aromatic C–H and C–O, respectively [14,15]. Fig. 2 presents that the FTIR spectra of Te/PBT and Co-Te/PBT nanocomposites are similar with that of neat PBT. However, the peak intensity at about of 500 cm^{-1} decreased in the case of nanocomposite, which might be due to the interaction of nanoparticles with PBT.

3.2. TGA study

Figs. 3 and 4 show the thermograms of PBT, Te/PBT and Co-Te/PBT nanocomposites. The thermogram of PBT presented that the degradation of polymer started at 370°C and almost completely degraded at 470°C. The

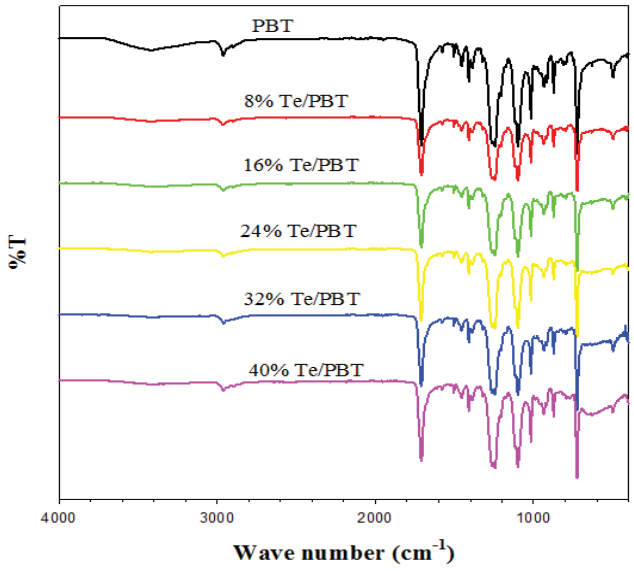

Fig. 1. Fourier-transform infrared spectra of neat PBT and different % of Te/PBT nanocomposites.

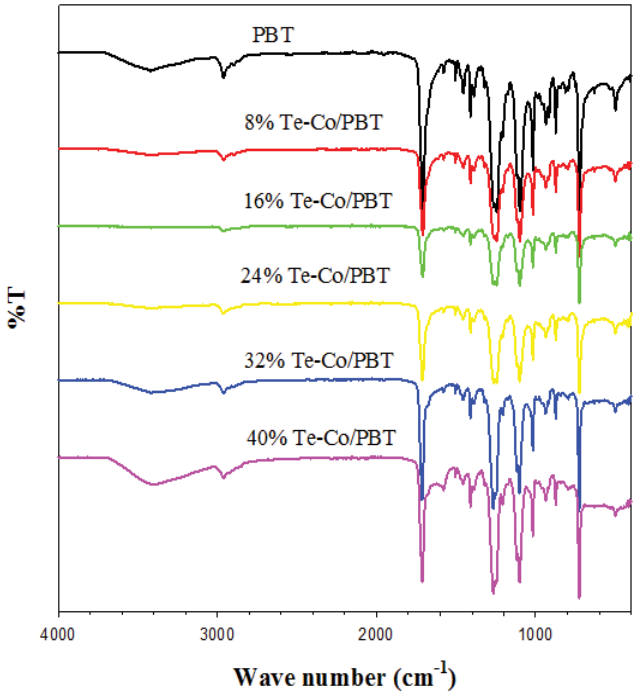

Fig. 2. Fourier-transform infrared spectra of neat PBT and different % of Te-Co/PBT nanocomposites.

thermogravimetric curve of Te/PBT showed that the degradation of nanocomposites are enhanced gradually as enhanced the quantity of Te NPs in the polymer matrix. The degradation of Te(8%)/PBT and Te(40%)/PBT were 385°C and 410°C, respectively. Similarly, the degradation of Co-Te/PBT nanocomposites is also increased gradually as increased the amount of Co-Te NPs in the matrix (Fig. 4). The degradation temperature of Co-Te(8%)/PBT and Co-Te(40%)/PBT were

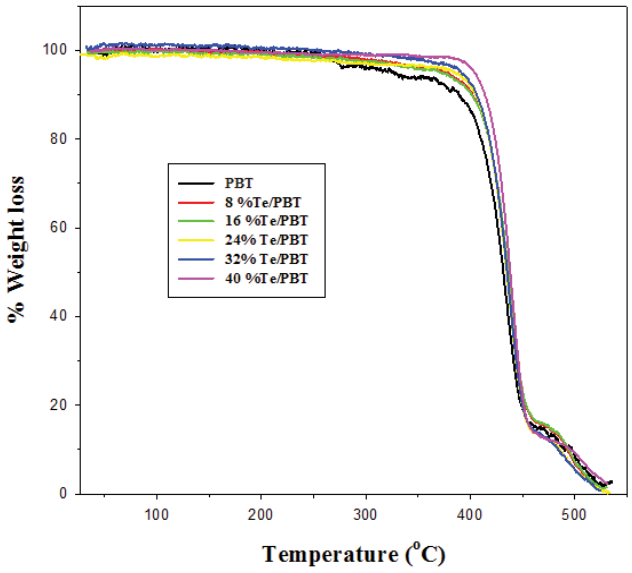

Fig. 3. Thermogravimetric analysis of different % of PBT and Te/PBT nanocomposites.

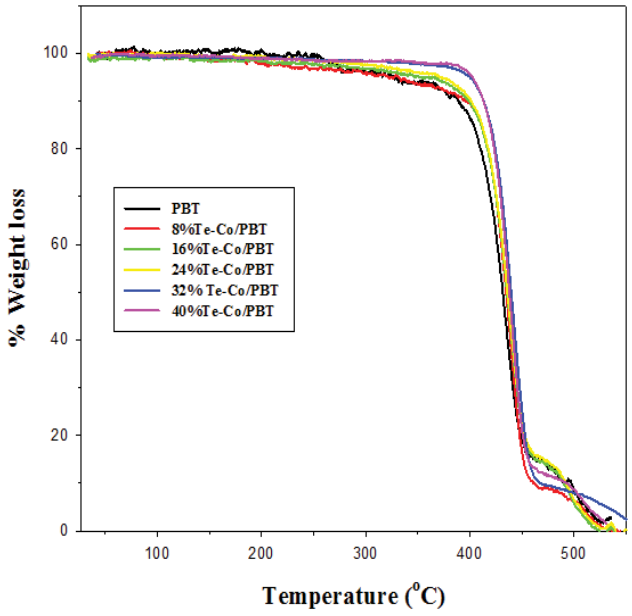

Fig. 4. Thermogravimetric analysis of different % of PBT and Te-Co/PBT nanocomposites.

about 380°C and 450°C, respectively. Similarly, Bhat et al. [16] also reported that the thermal stability of PVA/melamine formaldehyde polymer was significantly improved by the incorporation of NiO nanoparticles.

3.3. SEM study

Fig. 5 illustrates that the SEM images of cryofracture surfaces of Co(32%)/PBT and Te-Co(32%)/PBT nanocomposites. The SEM micrograph (Fig. 5b) presented that the Te NPs were present in dispersed form inside the PBT

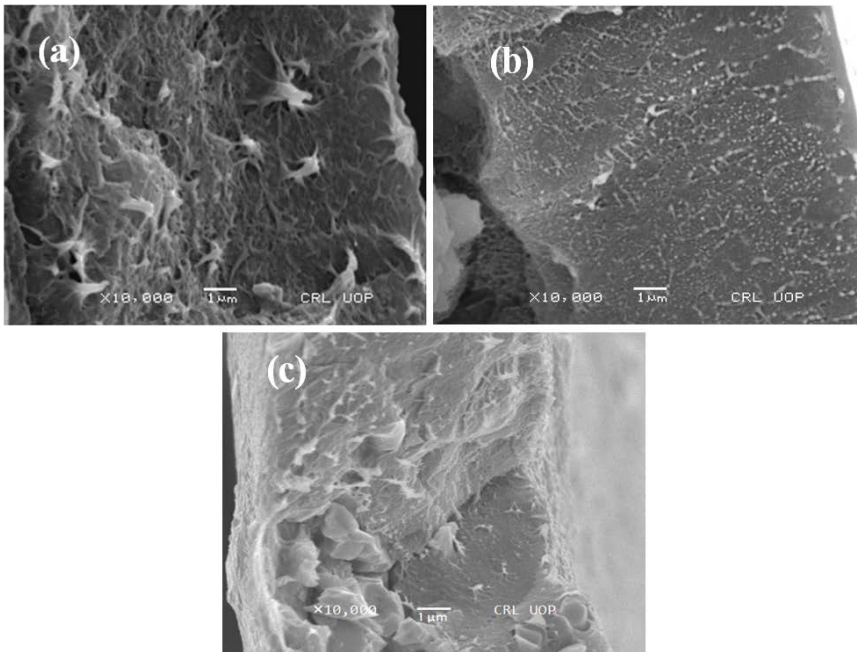

Fig. 5. Scanning electron micrographs of (a) PBT, (b) Te(32%)/PBT and (c) Te-Co(32%)/PBT nanocomposites.

matrix. It was also observed that the Te NPs are round in shape having size less than 150 nm. Similarly, Te-Co NPs is also present in dispersed form within the PBT matrix. The shapes of Te-Co NPs are also round with irregular shape.

3.4. EDX study

EDX technique is used in order to study the %composition of elements in a material/matrix. Fig. 6 shows the EDX spectra of PBT, Te/PBT and Te-Co/PBT nanocomposites, which illustrated that both Te and Co are present in PBT based nanocomposite. The spectra also presented a strong peak of Au, which came from gold coating during the analysis. Minute quantity of chloride is also found, which might remain from the precursor salt.

3.5. Photodegradation study of bromothymol blue

Fig. 7 presents the UV-Vis spectra of the BTB dye solution before and after UV irradiation as photodegraded by PBT and Te/PBT nanocomposites. The spectra showed that the degradation of BTB dye increased as increased the irradiation time. The spectra also presented that the photodegradation of dye increased as increased the quantity of Te NPs in PBT matrix.

Fig. 8 shows the comparison of % degradation of BTB, which was degraded by PBT and Te/PBT nanocomposite under UV irradiation at various time intervals. The results (Fig. 8) show that PBT degraded about 7% and 21% of dye within 2 and 8 h, respectively. While the Te(40 wt.%)/PBT nanocomposite degraded about 51% and 71% dye within 2 and 8 h irradiation time, respectively. Similarly, the increase of photodegradation of dye with high quantity of Fe_2O_3 NPs in polycaprolactone based nanocomposites was also reported by Saeed et al. [17].

3.6. Photodegradation of dye by Te-Co/PBT nanocomposite

Fig. 9 shows the UV-Vis spectra of the BTB dye solution before and after UV irradiation as photodegraded by PBT and Te-Co/PBT nanocomposites. The spectra presented that the degradation of BTB dye was increased as increased the irradiation time. The spectra also presented that the photodegradation of dye enhanced as increased the quantity of Te-Co NPs in polymer matrix. The results also showed that Te-Co(40 wt.%)/PBT nanocomposite degraded about 56% and 77% of dye within 2 and 8 h irradiation time, respectively (Fig. 10). It means that Te-Co/PBT nanocomposites are more active than Te/PBT composites. The comparison of current study results with reported results are shown in Table 1.

3.7. Effect of H_2O_2 on the photodegradation of BTB dye by PBT and nanocomposites

Tables 2 and 3 show the effect of H_2O_2 on the dye degradation, which presented that the BTB dye was significantly degraded by PBT and its nanocomposites when minute amount of H_2O_2 was added. In the presence of neat PBT, dye degradation was decreased gradually (40%, 38%, 35% and 30%) as increased as increased the amount of H_2O_2, that is, 0.005, 0.01. 0.02, and 0.03 mL, respectively within 1 min. Similarly, the degradation of BTB dye in the presence of Te(32%)/PBT and Te-Co(32%)/PBT nanocomposites were also decreased as increased the amount of H_2O_2. The decreased dye degradation with the increased amount of H_2O_2 might be due to the formation of $HO_2^{\bullet}$ radicals, which are less reactive radicals than the $OH^{\bullet}$ radicals and as result the rate of dye degradation is decreased [22].

$$H_2O_2 + {}^{\bullet}OH \rightarrow HO_2^{\bullet} + H_2$$

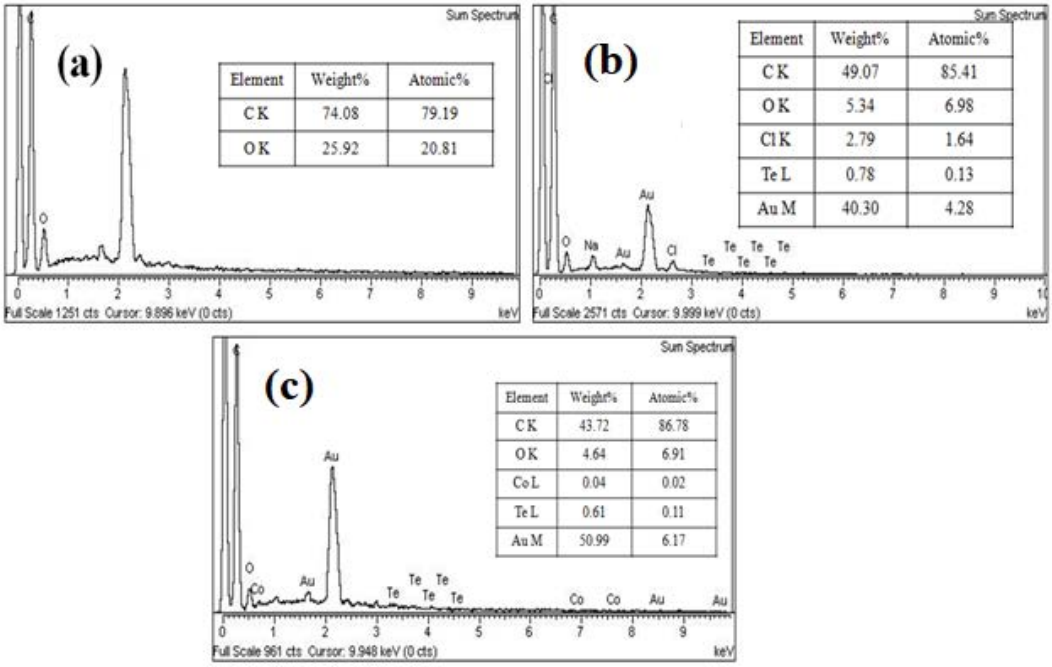

Fig. 6. Energy-dispersive X-ray spectra of (a) PBT, (b) Te/PBT and (c) Te-Co/PBT nanocomposites.

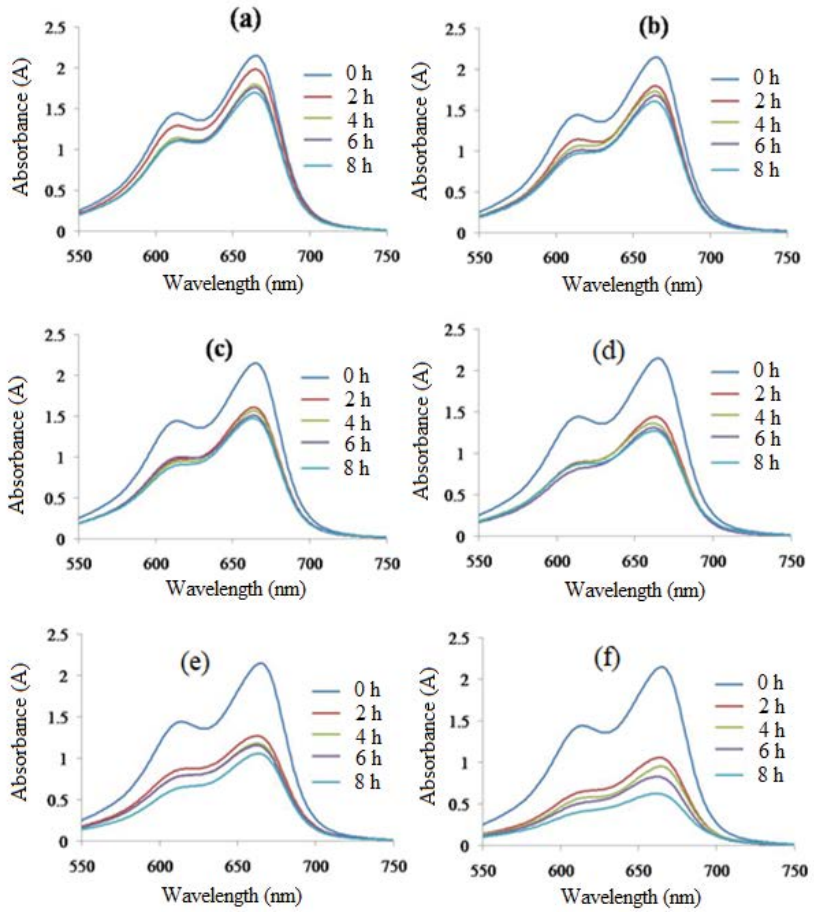

Fig. 7. UV-Vis spectra of BTB dye photodegraded by (a) neat PBT, (b) Te(8 wt.%)/PBT, (c) Te(16 wt.%)/PBT, (d) Te(24 wt.%)/PBT, (e) Te(32 wt.%)/PBT and (f) Te(24 wt.%)/PBT.

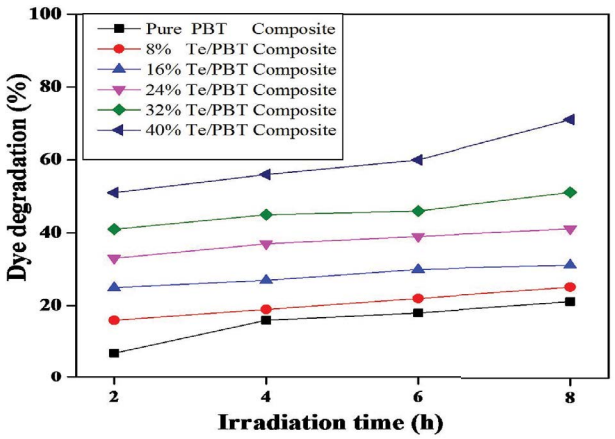

Fig. 8. % Degradation comparison of BTB by pure PBT and Te/PBT nanocomposites.

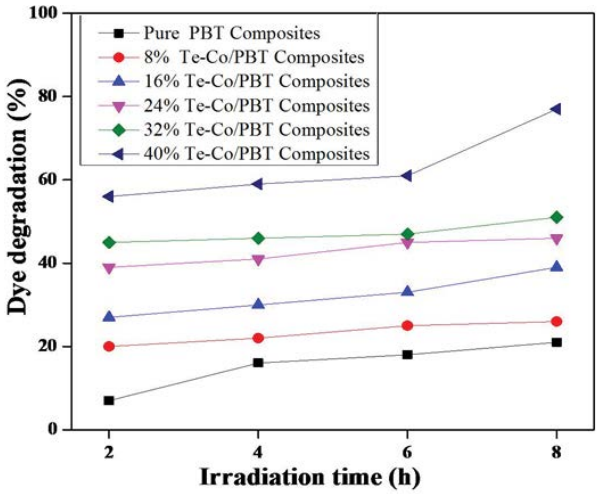

Fig. 10. % Degradation comparison of BTB by PBT and different percentages of Te-Co/PBT composites.

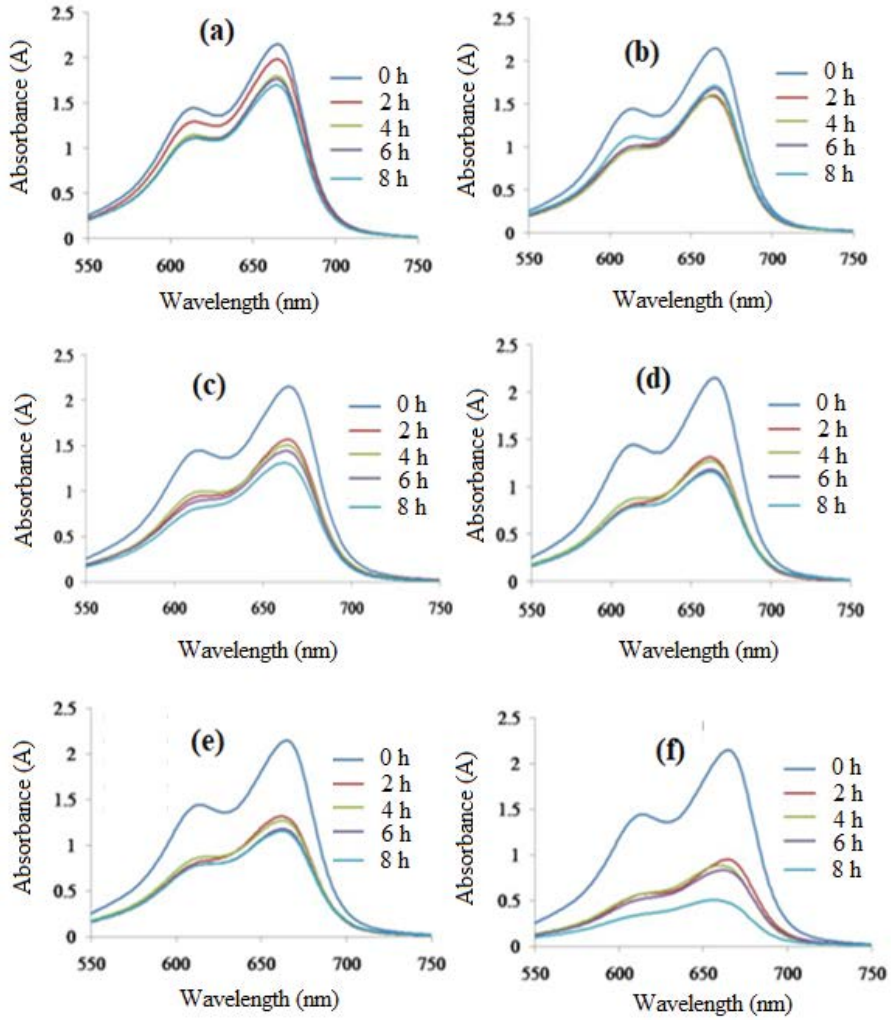

Fig. 9. UV-Vis spectra of BTB dye photodegraded by (a) PBT, (b) Te-Co(8 wt.%)/PBT, (c) Te-Co(16 wt.%)/PBT, (d) Te-Co(24 wt.%)/PBT, (e) Te-Co(32 wt.%)/PBT and (f) Te/Co(40 wt.%)/PBT.

Table 1
Comparison of current study with the reported results

Samples	Results	References
CuO	Less than 10% degradation	[18]
Lead complexes	47%–62% within 6 h	[19]
Selenium nanoparticles	62% within 1 h	[20]
Pd-γ-Al_2O_3	94% within 4 h	[21]
PdO-γ-Al_2O_3	52% within 4 h	
Te-Co(40 wt.%)/PBT	56% and 77% within 2 and 7 h, respectively	Current
Te(40 wt.%)/PBT	51% and 71% within 2 and 7 h, respectively	study

Table 2
Degradation of BTB dye by PBT and Te/PBT nanocomposites in the presence of H_2O_2

H_2O_2 (mL)	PBT (%)	Te(8 wt.%)/PBT (%)	Te(16 wt.%)/PBT (%)	Te(24 wt.%)/PBT (%)	Te(32 wt.%)/PBT (%)
0.005	40	46	50	77	78
0.01	38	45	48	71	75
0.02	35	43	45	59	72
0.03	30	39	41	50	69

Table 3
Degradation of BTB dye by PBT and Te-Co/PBT nanocomposites in the presence of H_2O_2

H_2O_2 (mL)	PBT (%)	Te-Co(8 wt.%)/PBT (%)	Te-Co(16 wt.%)/PBT (%)	Te-Co(24 wt.%)/PBT (%)	Te-Co(32 wt.%)/PBT (%)
0.005	40	46	42	45	51
0.01	38	45	30	41	55
0.02	35	43	33	34	51
0.03	30	39	35	39	44

4. Conclusion

The Te-PBT and Te-Co/PBT nanocomposites were prepared via solution casting method and were used as a photocatalyst for the degradation of BTB dye. Morphological study shows that the Te NPs were present in dispersed form inside the PBT matrix and are round in shape while in Te-Co/PBT nanocomposites, Te-Co NPs are found both in dispersed and agglomerated form inside the polymer matrix. The photodegradation study presented that the Te-PBT and Te-Co/PBT significantly degraded the BTB dye in aqueous medium. It was also found that the photodegradation ability of Te-Co/PBT was higher than Te/PBT. Further, the dye degradation was significantly increased (presence of nanocomposites films) as by the addition of small amount of H_2O_2.

References

[1] K. Saeed, M. Ishaq, Z.A. Shah, I. Ahmed, S. Ayaz, Effect of activated carbon on morphological, thermal and mechanical properties of polyvinyl chloride, Malaysian Polym. J., 10 (2015) 70–74.
[2] K. Saeed, I. Khan, Z. Ahmad, B. Khan, Preparation, analyses and application of cobalt-manganese oxides/nylon-6,6 nanocomposites, Polym. Bull., 75 (2018) 4657–4669.
[3] A. Ullah, Md. K. Haider, F.-F Wang, S. Morita, D. Kharaghani, Y. Ge, Y. Yoshiko, J.S. Lee, I.S. Kim, "Clay-corn-caprolactone" a novel bioactive clay polymer nanofibrous scaffold for bone tissue engineering, Appl. Clay Sci., 220 (2022) 106455, doi: 10.1016/j.clay.2022.106455.
[4] S.M. Thompson, M. Talò, B. Krause, A. Janke, M. Lanzerotti, J. Capps, G. Lanzara, W. Lacarbonara, The effect of branched carbon nanotubes as reinforcing nano-filler in polymer nanocomposites, Compos. Struct., 295 (2022) 115794, doi: 10.1016/j.compstruct.2022.115794.
[5] F. El-Sayed, V. Ganesh, M.S.A. Hussien, T.H. AlAbdulaal, H.Y. Zahran, I.S. Yahia, M.S. Abdel-wahab, M. Shakir, Y. Bitla, Facile synthesis of Y_2O_3/CuO nanocomposites for photodegradation of dyes/mixed dyes under UV- and visible light irradiation, J. Mater. Res. Technol., 19 (2022) 4867–4880.
[6] T. Gul, I. Khan, S. Ali, M. Sadiq, K. Saeed, Synthesis and characterization of Mn-Pt/AC nanoparticles and their photocatalytic and antibacterial applications, J. Dispersion Sci. Technol., 43 (2022) 612–619.
[7] K. Saeed, I. Khan, S.-Y. Park, TiO_2/amidoxime-modified polyacrylonitrile nanofibers and its application for the photodegradation of methyl blue in aqueous medium, Desal. Water Treat., 54 (2015) 3146–3151.
[8] M. Sajjadi, M. Nasrollahzadeh, M.R. Tahsili, Catalytic and antimicrobial activities of magnetic nanoparticles supported *N*-heterocyclic palladium(II) complex: a magnetically recyclable catalyst for the treatment of environmental contaminants in aqueous media, Sep. Purif. Technol., 227 (2019) 115716, doi: 10.1016/j.seppur.2019.115716.

[9] X. Wang, X. Fang, X. Yuan, F. Zhang, J. Yang, N. Ling, H. Yang, Synthesis, structure and photocatalytic properties of two novel Cd(II) coordination polymers based on 1-[(2-methyl-1H-benzoimidazol-1-yl) methyl]-1H-benzotriazole, J. Mol. Struct., 1255 (2022) 132436, doi: 10.1016/j.molstruc.2022.132436.
[10] B. Jones, D. Mafukidze, T. Nyokong, Fabrication of electrospun fibers from a porphyrin linked to polyacrylonitrile polymer for photocatalytic transformation of phenols, J. Mol. Struct., 1213 (2020) 128191, doi: 10.1016/j.molstruc.2020.128191.
[11] B. Neppolian, H.C. Choi, S. Sakthivel, B. Arabindoo, V. Murugesan, Solar/UV-induced photocatalytic degradation of three commercial textile dyes, J. Hazard. Mater., 89 (2002) 303–317.
[12] M. Saeed, K. Albalaw, I. Khan, N. Akram, I.H.A. Abd El-Rahim, S.K. Alhag, A.E. Ahmed, Faiza, Synthesis of p-n NiO-ZnO heterojunction for photodegradation of crystal violet dye, Alexandria Eng. J., 65 (2023) 561–574.
[13] A. Morfin-Gutierrez, J.L. Sanchez-Orozco, L.A. García-Cerda, B. Puente-Urbina, H.I. Mel'endez-Ortiz, Synthesis and characterization of poly(N-vinycaprolactam)-grafted gold nanoparticles by free radical polymerization for using as chemotherapeutic delivery system, Mater. Chem. Phys., 266 (2021) 124535, doi: 10.1016/j.matchemphys.2021.124535.
[14] E.D. Tsochatzis, J.A. Lopes, M.V. Holland, F. Reniero, C.G.H. Emons, Isolation, characterization and structural elucidation of polybutylene terephthalate cyclic oligomers and purity assessment using a ^{1}H qNMR method, Polymers, 11 (2019) 464, doi: 10.3390/polym11030464.
[15] H. Zhang, S. Sun, M. Ren, Q. Chen, J. Song, H. Zhang, Z. Mo, Thermal and mechanical properties of poly(butylene terephthalate)/epoxy blends, J. Appl. Polym. Sci., 109 (2011) 4082–4088.
[16] S.A. Bhat, F. Zafar, A.U. Mirza, A.H. Mondal, A. Kareem, Q.M.R. Haq, N. Nishat, NiO nanoparticle doped-PVA-MF polymer nanocomposites: preparation, Congo red dye adsorption and antibacterial activity, Arabian J. Chem., 13 (2020) 5724–5739.
[17] K. Saeed, N. Khan, T. Shah, M. Sadiq, Morphology, properties and application of iron oxide/polycaprolactone, J. Chem. Soc. Pak., 43 (2021) 34–40.
[18] S. Prakash, N. Elavarasan, A. Venkatesan, K. Subashini, M. Sowndharya, V. Sujatha, Green synthesis of copper oxide nanoparticles and its effective applications in Biginelli reaction, BTB photodegradation and antibacterial activity, Adv. Powder Technol., 29 (2018) 3315–3326.
[19] A.E. Oluwalana, P.A. Ajibade, Structural, optical and photocatalytic studies of hexadecylamine-capped lead sulfide nanoparticles, Int. J. Ind. Chem., 11 (2020) 249–260.
[20] A. America, M. Shakibaieb, A. Americ, M.A. Faramarzid, B.A. Heidarib, H. Forootanfar, Photocatalytic decolorization of bromothymol blue using biogenic selenium nanoparticles synthesized by terrestrial actinomycete *Streptomyces griseobrunneus* strain FSHH12, Desal. Water Treat., 57 (2016) 21552–21563.
[21] A.P. Kumar, D. Bilehal, A. Tadesse, D. Kumar, Photocatalytic degradation of organic dyes: Pd-gAl_2O_3 and PdO-γ-Al_2O_3 as potential photocatalysts, RSC Adv., 11 (2021) 6396–6406.
[22] M.A. Behnajady, N. Modirshahla, M. Shokri, Photodestruction of Acid Orange 7 (AO7) in aqueous solutions by UV/H_2O_2: influence of operational parameters, Chemosphere, 55 (2004) 129–134.